Long Tailed Maps as a Representation of Mixed Mode Oscillatory Systems

Rajesh Raghavan[2] and G. Ananthakrishna[1,2]
[1] Materials Research Centre
Indian Institute of Science
Bangalore 560012, India

and
[2] Center for Condensed Matter Theory
Indian Institute of Science
Bangalore 560012, India

Mixed mode oscillatory (MMO) systems are known to exhibit some generic features such as the reversal of period doubling sequences and crossover to period adding sequences as bifurcation parameters are varied. In addition, they exhibit a nearly one dimensional unimodal Poincare map with a longtail. We recover these common features from a general class of two parameter family of one dimensional maps with a unique critical point that satisfy a few general constraints that determine the nature of the map. We derive scaling laws that determine the parameter widths of the dominant windows of periodic orbits sandwiched between two successive states of RL^k sequence. An example of a two parameter map with a unique critical point is introduced to verify the analytical results.

PACS numbers: 82.40Bj, 05.45Ac

I. INTRODUCTION

Dynamical systems with disparate time scales for the participating modes often exhibit periodic states characterised by a combination of relatively large amplitude and nearly harmonic small amplitude oscillations. Such periodic states, called the mixed mode oscillations (MMOs), and the associated complex bifurcation sequences have been observed in models and experiments in the area of chemical kinetics [1, 2, 3, 4, 5], electrochemical reactions [6, 7, 8], biological systems [9], and in many physical systems [10, 11, 12]. These MMO systems typically exhibit the following features - (a) period doubling (PD) sequences and their reversal in multi-parameter space with respect to a primary bifurcation parameter keeping other parameters fixed, and (b) crossover to bifurcation sequences of alternate periodic-chaotic windows when one of the secondary bifurcation parameters is varied wherein dominant windows of periodicity increase in an arithmetical order which we refer to as period adding (PA) sequences [3, 4, 6, 7, 8, 12, 13].

As an illustration of the generic features of MMO systems, we collect some relevant results from our earlier study [12, 14] on Ananthakrishna's model (AK model) for a type of plastic instability [15]. As in other MMO systems, this model also involves disparate time scales. The bifurcation portraits (with respect to a primary bifurcation parameter, e) of the model show period doubling sequences and their reversal, gradually changing over to period adding sequences as the secondary bifurcation parameter, m, is increased. (See Fig. 1a,b.) As can be seen in Fig. 1b, the dominant periodic orbits of 1^s kind constitute the period adding sequence. (Here, we use the conventional notation of L^s to represent period orbits in MMO systems where L and s correspond to large and small amplitude oscillations respectively.) In the parameter space, wherein the reversal of period doubling sequences occur, periodic adding sequences are finite. Periodic orbits of 1^s type loose their stability in a period doubling bifurcation as the (primary) control parameter is increased, restabilize through a reverse period doubling bifurcation, and are eventually annihilated in a fold bifurcation [12]. In this parameter range, we have also studied the next maximal amplitude (NMA) maps [16] obtained by plotting one maxima of the evolution of the fast variable with the next [14]. (The NMA maps can be regarded as a specific form of the Poincare maps.) These NMA maps show a near one dimensional unimodal nature with features of sharp maximum and a long tail. The sharpness of the NMA maps increases with the primary bifurcation parameter for a fixed value of the secondary bifurcation parameter. (See Fig. 2a and 2b. Also, see [14, 17].) Several other MMO systems also exhibit similar features.

A well studied example of MMO systems is the Belusov Zhabotansky (BZ) reaction system. Exhaustive theoretical/experimental studies for the BZ systems in two parameter space have shown that the NMA maps of these systems have a unimodal structure with a long tail and show a similar trend as a function of the control parameters [5, 13, 18] as in the case of AK model. Other MMO systems which display similar features include lasers with a saturable absorber, autocatalytic systems and a number of oscillating chemical reaction systems [4, 11, 13, 19].

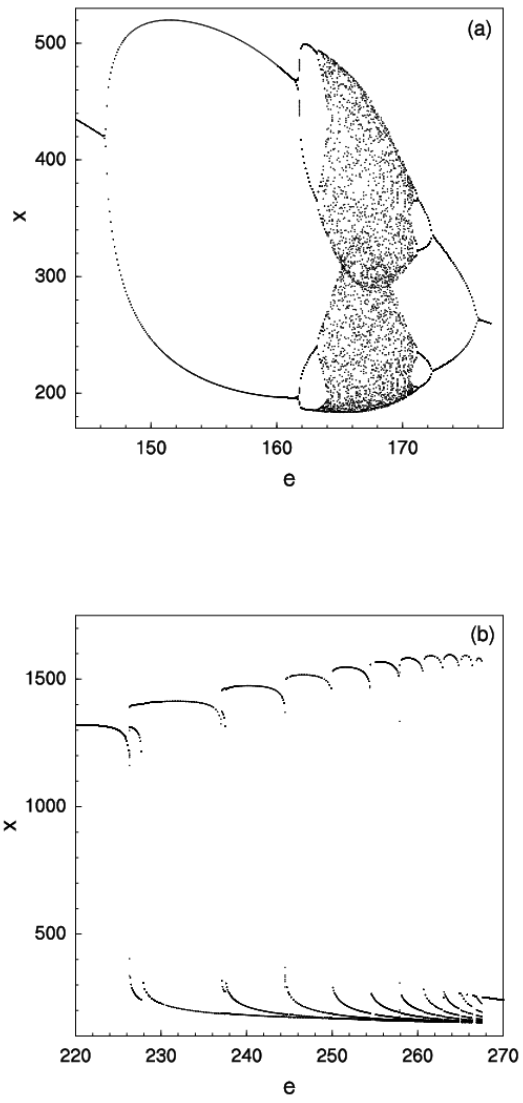

FIG. 1: Bifurcation diagrams for the AK model for a plastic instability with primary bifurcation parameter, e and secondary bifurcation parameter, m. (a) Cascading period doubling bifurcations and their reversals forming a bubble structure for $m = 2.16$, and (b) period adding sequences for $m = 1.2$. Chaotic regions exists in a vanishingly small parameter regions sandwiched between successive 1^s periodic states.

The periodic states representative of MMO systems have been shown to be associated with systems exhibiting global bifurcations in the form of approach to homoclinicity [20, 21, 22, 23]. Although, a variety of tools are available for the study of bifurcations in dynamical systems, understanding these features of MMOs has not been easy mainly due to the lack of adequate analytical tools to handle the global nature of bifurcations underlying the MMOs. However, since information regarding the nature and properties of periodic orbits of continuous flow systems are known to be embedded in Poincare maps, they have been used effectively to understand the underlying bifurcation mechanisms [16, 20, 24, 25]. For instance, considerable insight has been obtained through the Poincare maps derived from approach to homoclinicity [20, 21, 22, 23]. Since, most of the MMO systems exhibit high dissipation, there have been attempts to understand the dynamical behaviour of MMO system (specifically BZ system) by modelling its NMA maps as one dimensional discrete dynamical systems [18, 26, 27, 28, 29].

The two distinct bifurcation features, namely, the reversal of bifurcation sequences and the period adding sequences have been modelled separately using one dimensional maps. For instance, of the many mechanisms suggested for the reversal of period doubling sequences, a simple one involves maps having a single critical point along with nonmonotonous dependence of the control parameter [30]. Another one is a unimodal map having a negative Schwarzian derivative [31]. Yet another one involves a competition between more than one critical point in the dynamics of the map [32, 33, 34]. It has also been shown that the transmutation of the U-sequences to the Farey sequences or specifically, its subset, the period adding sequences can arise in maps with *more than one critical point* with multiple parameters[35]. However, to the best of author's knowledge, *none of these mechanisms apply* to experimental and model MMO systems where one finds Poincare maps with unique critical point as well as smooth crossover from period doubling and its reversal to Farey sequences for a monotonous change in a secondary bifurcation parameter. There has been no explanation for this crossover as well. *Here, we show that a general class of maps with a unique critical point satisfying some broad constraints can show a gradual change from bifurcation diagrams having the reversal of the period doubling sequences to period adding sequences for a smooth change of parameters.*

To achieve this objective, we first abstract common features of MMO systems, and then impose them in the form of some general constraints on one dimensional maps with two bifurcation parameters in an effort to understand the above dynamical features of the MMO systems. (Note that almost all MMO systems have two or more parameters.) Using these general constraints, we first analyse the basic mechanism responsible for the reversal of periodic sequences of RL^k type which correspond to the dominant 1^s sequence in MMO systems. (Admittedly, this is a much less difficult issue than the origin of reversal of all the bifurcation sequences in these maps.)

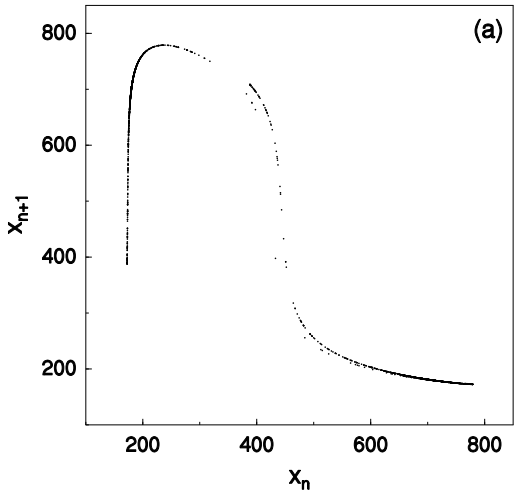

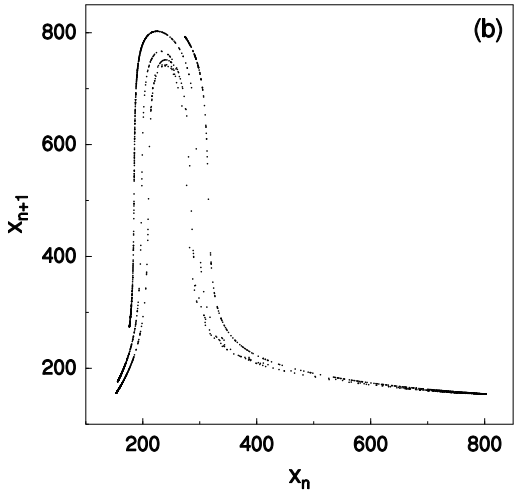

FIG. 2: Poincare maps from the AK model for $m = 1.8$ and (a) $e = 190.6$, and (b) $e = 202.7$. (Multiple folds arise as a result of finite dissipation.)

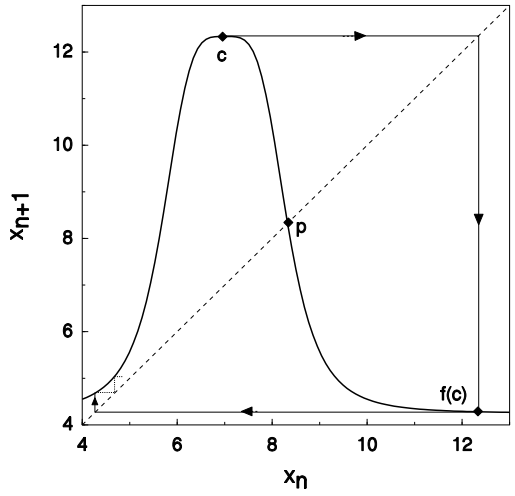

FIG. 3: Typical structure of the map-L described in appendix for $\mu = 4.0$ and $\xi = 18.0$. The period one fixed point(p), critical point c and the first iterate $f(c)$ are also indicated.

We also show that the windows of symbolic sequence RL^k are the dominant windows in the parameter space and derive scaling relations for the onset of windows of periodic orbits sandwiched between successive windows of RL^k sequence. The so derived *scaling relations relate the slopes near the critical point and unstable fixed point, and are unlike the usual scaling relations derived in terms of bifurcation parameters.* Investigation of the reversal of PD sequences in turn allows us to understand the mechanism for the onset of the period adding sequences as well. *Our analysis shows that the eigen value of the unstable fixed point of the map plays a fundamental role in controlling the window widths of the periodic orbits as a function of the control parameter in the family of long tailed maps.* Hence, the geometrical shape of the map determined by the nature of unstable fixed point and the long tail structure is shown to be the underlying factor for the period adding bifurcation sequences. (For this reason, we refer to these general class of maps as *long tailed maps.*)

We verify these scaling relations by constructing an example of a two parameter family of one dimensional maps with a geometrical shape similar to the NMA maps of MMO systems having a long tail. This example map, referred to as map-L, exhibits a smooth transition from period doubling bifurcation sequences and their reversals to period adding sequences for a variation of a secondary bifurcation parameter (Appendix). We emphasise that the example map-L is primarily introduced as an aid to verify the analytical results. However, to pin down the ideas, it will be useful to refer to the geometrical shape of map-L (Fig. 3) which is seen to be similar to Fig. 1. Finally, we discuss the results and the correspondence with the continuous flow dynamical systems having a finite dissipation.

II. DYNAMICS OF THE LONG TAILED MAPS

In this section, , we first attempt to extract conditions that needs to imposed on one dimensional maps by studying MMO systems with generic features mentioned in Introduction section *without any reference to any*

functional form for the map. These conditions, stated below, are motivated by the study of the long tailed maps of MMO systems and are further aided by our detailed studies on the AK model [12, 14]. Before doing so, we first attempt to capture the connection between periodic orbits of MMO systems and one dimensional maps. For the sake concreteness, we use Shilnikov scenario where the homoclinic contact is with respect to a saddle focus and motivate the issues using known facts of the AK model studied in detail [12, 14, 17].

We first identify the equilibrium saddle fixed point of a MMO system, as in the case of the AK model, with the origin of the map. In many of these experimental and model systems, interesting dynamics arises in the region between the first Hopf bifurcation resulting from destabilization of the fixed point and the restabilization of the fixed point from the periodic orbit through a reverse Hopf bifurcation. This is identified with back-to-back Hopf bifurcation as in the case of the AK model also [4, 7, 11, 36]. The principal periodic orbit (PPO) born out of a Hopf bifurcation is identified fixed point p of the map (see for instance Fig. 3). Further, careful observation of the bifurcation diagrams of MMO systems show that the complex bifurcation sequence occurs in the region of the parameter where the amplitude of the PPO decreases and approaches the reverse Hopf bifurcation point as the bifurcation parameter is increased[4, 7, 11, 12]. This implies that the fixed point moves toward the origin of the map. As the complex dynamics is terminated by a reverse Hopf bifurcation as the parameter is increased, the height of the map also decreases as a function of a parameter which we identify as the primary control parameter, μ. These two statements can be written as two conditions [49]:

$$\frac{\partial f}{\partial \mu}(x) < 0, \tag{1}$$

$$|\frac{\partial f}{\partial \mu}(c)| < |\frac{\partial f}{\partial \mu}(p)|. \tag{2}$$

where c is the maximal point of the map. We expect that these conditions are satisfied by either of the two parameters of the two parameter family of maps. Without loss of generality, we identify the parameter, μ, in Eq. 1 and 2 as the primary bifurcation parameter. (We shall use ξ for the secondary bifurcation parameter.) Here, we note that Eq. 2 implies that the map becomes increasingly sharp as μ is increased. As a consequence, the map also develops a long tail. Since, in most cases, the variables of continuous time systems are positive, we have taken the NMA maps to be limited to positive values. In Shilnikov scenario, as the orbit is reinjected close to the origin, the orbit spiral out along the unstable manifold. Closer the reinjection to the saddle focus, larger are the number of small amplitude oscillations. This can be captured by ensuring an intermittency channel in the one dimensional map. To mimic reinjection of the phase space orbit close to the saddle focus fixed point, we require $f(0, \mu, \xi) = a$ and $f(x, \mu, \xi) \to a' < a$ for large x, where a and a' are non zero positive constants. Further, since we are interested in maps with unique critical point c, there are two monotonic branches to the left and right of c. Further, as the whole map is coming down as a function of μ, the existence of a intermittency channel to left of c, should be anticipated. (Such a channel is actually observed in many systems [4, 7, 8, 12, 13].) This channel is ensured if we impose

$$f'(0, \mu, \xi) < 1 \tag{3}$$

$$f''(0, \mu, \xi) > 0. \tag{4}$$

The above conditions (Eqs. 1-4) are equivalent to the observed features (a) to (c) of MMO systems as mentioned in the appendix. We shall, henceforth, refer to *the general class of maps determined by these few constraints (Eqs. 1-4) as long tailed maps.*

To fix up the preliminaries, we start with some notations and definition. For the sake of brevity, wherever necessary, we will use $f(x)$ in place $f(x; \mu, \xi)$. The $n-$th iterate of x is denoted by $f^n(x) = f(f^{n-1}(x)) = f \circ f^{n-1}(x)$. The iterates of $f(x; \mu, \xi)$ are given by $\theta : \{x_0, x_1, x_2, \cdots, x_n, \cdots\}$ with the respective neighbourhoods given by $\{I_0, I_1, I_2, \cdots, I_n, \cdots\}$, where $x_n \in I_n$. A point q is k-periodic if $f^k(q; \mu, \xi) = q$, while $f^i(q; \mu, \xi) \neq q$ for $0 < i < k - 1$. In particular, we denote the period one fixed point by p. The eigen value of a k-period cycle q is $\frac{\partial f^k}{\partial x}(q) = \lambda$. If $|\lambda| < 1$, then q is stable. Further, we will always choose the initial point, x_0, to be the iterate that is closest to the critical point in the stable periodic window. Finally, we will deal with the nontrivial dynamics of the map in the interval $I = [c_1, c_0]$, where $f(c) = c_0$ and $f^2(c) = c_1$. Hereafter, we refer to the parameter windows of stable periodic orbits using the corresponding symbolic dynamics notation. (In this notation, to conform with the conventional representation, the symbol corresponding to the initial iterate x_0 has been dropped. For example, we represent the entire period three window by simply RL.)

A rough understanding of the reversal of the period doubling sequences can be obtained by examining the changes in the stability of p. For a unimodular map, Eq.(2) implies that as μ is increased, as the fixed point p moves towards the origin, it loses stability leading to the first period doubling (PD) bifurcation, say at $\mu = \mu_2$. On the other hand, Eq.(1) implies the map as a whole is coming down which in turn means that p moves towards the critical point, c, as a function of μ. Once p crosses the point of inflection, $\frac{\partial f}{\partial x}(p)$ increases eventually culminating in a stable monoperiodic orbit when $\frac{\partial f}{\partial x}(p) > -1$, say at $\mu = \mu_2'$. Thus, if there are period doubling sequences beyond $\mu = \mu_2$, then their reversal has to occur within the parameter range μ_2 and μ_2'.

Since the map is comes down as a function of μ, there are two possibilities for reinjection, namely $f^2(c)$ falls to

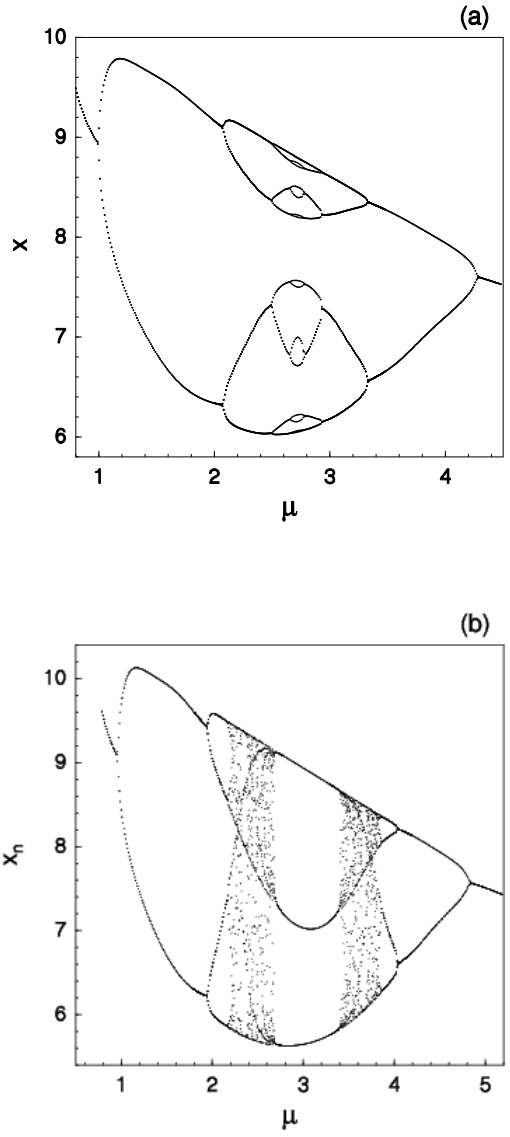

FIG. 4: Bifurcation diagrams for the Map-L. (a) Cascading period doubling with a bubble structure for $\xi = 11.415$, and (b) Bubble structure with dominant period three window for $\xi = 11.43$.

right of a point $x = x_t$ at which $f'(x_t, \mu, \xi) = 1$ and $f^2(c)$ falls to its left. The latter clearly corresponds to the realization of period adding sequences. Any further increase in the parameter creates two more fixed points on the ascending branch of the map.

A. Reversal of bifurcation sequences

Before we proceed further, we give below some derivatives which will be used to establish subsequent results. Using the chain rule for iterates of maps, we have

$$\frac{\partial f^n}{\partial x}(x_0) \;=\; \prod_{i=0}^{n-1} \frac{\partial f}{\partial x}(f^i(x_0)). \tag{5}$$

Using Eq. (5), we can write

$$\begin{aligned}\frac{\partial^2 f^n}{\partial x^2}(x_0) \;&=\; \frac{\partial}{\partial x}\left(\frac{\partial f^n}{\partial x}(x_0)\right), \\ &=\; \sum_{k=0}^{n-1}\left(\frac{\frac{\partial^2 f}{\partial x^2}(f^k(x_0))}{\frac{\partial f}{\partial x}(f^k(x_0))}\right)\prod_{j=0}^{n-1}\frac{\partial f}{\partial x}(f^j(x_0)).\end{aligned} \tag{6}$$

Similarly, the parameter dependence of the iterates lead to

$$\frac{df^n}{d\mu}(x) \;=\; \frac{\partial f}{\partial \mu}(f^{n-1}(x)) + \frac{\partial f}{\partial x}(f^{n-1}(x))\frac{\partial f^{n-1}}{\partial \mu}(x). \tag{7}$$

In order to understand the mechanism of reversal of period doubling sequences exhibited by the unimodal long tailed maps, we restrict our discussion to a simpler problem namely, the reversal of period doubling of the dominant sequences of the type RL^k. (We will soon argue that these type of periodic orbits are the dominant ones.)

To pin down the ideas, consider the map-L which satisfies the requirement of the long tailed maps. The dominance of the RL^k periodic orbits are well visualised in the bifurcation diagrams of map-L (Fig. 5a). A prominent feature of the bifurcation diagram is the presence of relatively dark bands of iterates (corresponding to superstable orbits) that run across the bifurcation diagram connecting successive RL^k periodic windows. (Similar features are routinely observed in bifurcation diagrams of MMO systems also.) These bands arise as a consequence of the increased stability of the iterates closer to the critical point of the map. It is clear that these bands share a similar sequential structure of iterates as the RL^k sequence, specifically the superstable point of the periodic orbit lies on the envelope of these bands. In the following analysis and later, we utilise this contiguous nature of envelope of bands to determine the parametric dependence of iterates.

Consider the n iterates of $k+2$ periodic cycle which consists of one visit to the right of the critical point, c, and k visits to the monotonically increasing arm of the map. We examine the reversal of the sign of Eq.(7) as μ is increased for periodic orbits of the form RL^k as the reversal of the periodic sequence is assured if $\frac{\partial f^2}{\partial \mu}(x_0)$ changes sign at $\mu = \mu_{r_2}$. To do this, first consider the second iterate ($n = 2$) of Eq.(7). Using $x_0 = c$, we get

$$\frac{\partial f^2}{\partial \mu}(c) = \frac{\partial f}{\partial \mu}(f(c)) + \frac{\partial f}{\partial x}(f(c))\frac{\partial f}{\partial \mu}(c). \tag{8}$$

Equation (1) implies that the first term on the RHS of Eq.(8) is negative while the second term is positive

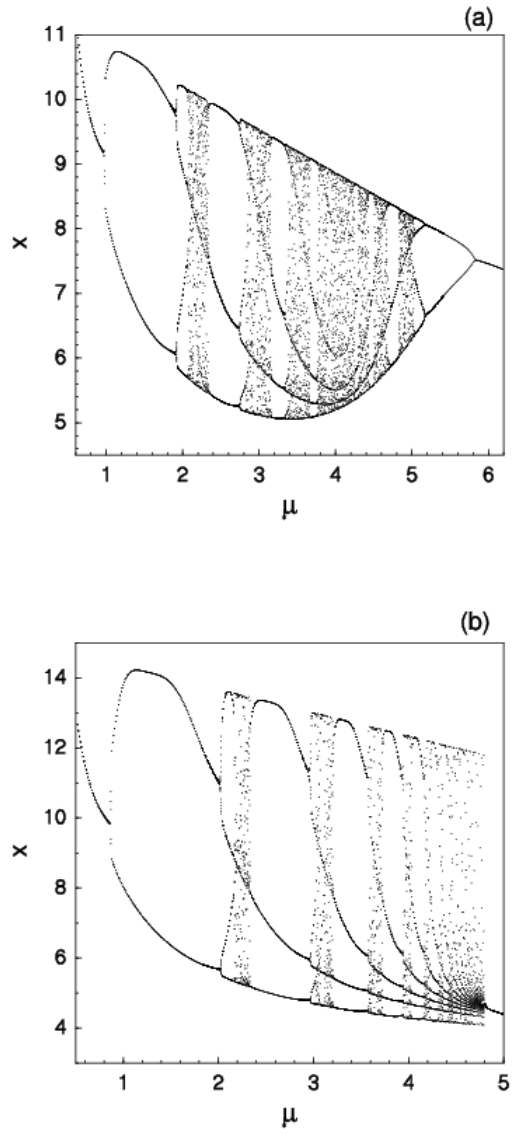

FIG. 5: The bifurcation diagrams for Map-L. (a) period adding sequence coexisting with reversal of period doubling sequences at $\xi = 12.8$, and (b) period adding sequence with fold bifurcation at the accumulation point of RL^n periodic windows for $\xi = 18.0$. Note the similarity with Fig. 1 b.

since $\frac{\partial f}{\partial x}(f(c))$ and $\frac{\partial f}{\partial \mu}(f(c))$ are negative. However, initially, $|\frac{\partial f}{\partial x}(f(c))|$ *is small as* $f(c)$ *refers to the tail part*, and hence there is a region of μ for which $|\frac{\partial f}{\partial \mu}(f(c))| > |\frac{\partial f}{\partial x}(f(c))\frac{\partial f}{\partial \mu}(c)|$ and thus, LHS of Eq.(8) is negative. As μ is increased (as $f(c)$ moves up towards c), $|\frac{\partial f}{\partial x}(f(c))|$ increases and $\frac{\partial f^2}{\partial \mu}(c)$ turns positive, say at $\mu = \mu_{r_2}$. (Note that the value of μ_{r_2} is in principle a function of ξ. For example, in the case of map-L, for $\xi = 11.0$, $\frac{\partial f^2}{\partial \mu}(c)$ changes sign at $\mu \sim 2.2$.) Beyond $\mu = \mu_{r_2}$,$\frac{\partial f^2}{\partial \mu}(c)$ increases with μ.

Now, consider evaluating Eq.(7) for successive $n > 2$. Consider,

$$\frac{\partial f^3}{\partial \mu}(c) = \frac{\partial f}{\partial \mu}(f^2(c)) + \frac{\partial f}{\partial x}(f^2(c))\frac{\partial f^2}{\partial \mu}(c) \qquad (9)$$

For periodic orbits of type RL^k, $\frac{\partial f}{\partial x}(f^2(c)) > 0$, and from Eq. (1), $\frac{\partial f}{\partial \mu}(f^2(c)) < 0$. Further, from the previous discussion, since $\frac{\partial f^2}{\partial \mu}(c)$ is zero at $\mu = \mu_{r_2}$, LHS of Eq.(9) negative at this value. As μ is increased, $\frac{\partial f^2}{\partial \mu}(c)$ turns positive and the second term on the RHS of Eq.(9) is an increasing function of μ. Thus, the LHS which is negative for $\mu < \mu_{r_2}$ becomes positive at some value $\mu = \mu_{r_3} > \mu_{r_2}$. In addition, note that $|\frac{\partial f^3}{\partial \mu}(c)| > |\frac{\partial f^2}{\partial \mu}(c)|$ around $\mu = \mu_{r_3}$. Similar arguments can be used to show that $\frac{\partial f^n}{\partial \mu}(c)$, which is negative for $\mu < \mu_{r_{n-1}}$ will change sign at $\mu = \mu_{r_n}$. Thus, the reversal of successive periodic orbits occur at increasing values of parameter given by

$$\mu_{r2} < \mu_{r3} < \mu_{r4} < ...$$

(Note that these results are largely a consequence of Eqs.(1) and (2).) These results can be verified from the bifurcation portraits of map-L shown in Fig. 5a. Changes in sign of $\frac{\partial f^n}{\partial \mu}(c)$, manifest as changes in the sign of the slope of the envelope of superstable iterates with parameter. It is clear that lower outermost envelope corresponding to the third iterate of critical point changes the sign of slope first, signalling the onset of reversal of the periodic sequence.

A natural consequence of the reversal of periodic orbits is the presence of isolated bifurcation curves or the isolas. In the following, we trace the origin of of isolas using the first two constraints (Eqs. 1,2) on the general class of maps. Again, we restrict our attention to periodic orbits of the form RL^k. Consider using $x_0 = c$ in Eq.(6) for an allowed k-periodic RL^{k-2}, we get

$$\begin{aligned}\frac{\partial^2 f^k}{\partial x^2}(c) &= \frac{\partial^2 f}{\partial x^2}(c)\prod_{n=1}^{k-1}\frac{\partial f}{\partial x}(x_n) \\ &= \frac{\partial^2 f}{\partial x^2}(c).\frac{\partial f}{\partial x}(f(c)).\prod_{n=2}^{k-1}\frac{\partial f}{\partial x}(x_n)\end{aligned}$$

We first note that excepting $\frac{\partial f}{\partial x}(f(c))$ and $\frac{\partial^2 f}{\partial x^2}(c)$, all other terms are positive. Thus, as the visits are to the left of c, the sign of $\frac{\partial^2 f^k}{\partial x^2}(c)$ is positive for all allowed values of μ. This positive curvature of the map and its parametric dependence, $\frac{\partial f^k}{\partial \mu}(c) < 0$ for $\mu < \mu_{r_k}$, implies that a k-periodic orbit is created due to a tangent bifurcation as μ is increased. For further increase in μ, $f^k(c)$ comes down, triggering a period doubling bifurcation making the periodic orbit unstable.

Increasing μ beyond μ_{r_k} reverses the period doubling since $\frac{\partial f^k}{\partial \mu}(c)$ becomes positive, ie., the region around c of $f^k(x)$ moves up eventually restabilizing the $k-$th periodic orbit. Further increase in μ destroys the stable periodic orbit in another tangent bifurcation (see Fig. 5b). The creation of a periodic orbit, its destabilization and restabilization, followed by its destruction constitutes an isolated bifurcation curve (isola). This happens for each of the allowed periodic orbit of the form RL^k. From these arguments, it is clear that the isola corresponding to the smallest allowed period orbit contains all isolas of the allowed periodic orbits of larger k, with the smallest one being the maximum periodic orbit. In addition, there exists a maximum periodic orbit of RL^k that is allowed. In the case of map-L, it is clear that the value at which different iterates show reversal in sign $\frac{\partial f^n}{\partial \mu}(c)$ are different as can be seen from Fig. 5a and the reversal of all the allowed periodic orbits of RL^k type occurs beyond $\mu \sim 4.05$ ($\xi = 8.0$) and the maximum allowed periodic sequence period five ($k = 3$). Indeed, similar isola features are well documented in bifurcation diagrams of MMO systems[4, 12].

It is possible to extend these arguments to some other sequences of periodic orbits as well. For example, consider periodic orbits of RL^kR^{2m} type. Similar arguments as before show that $\frac{\partial^2 f^{k+2(m+1)}}{\partial x^2}(c)$ is positive and $\frac{\partial f^{k+2(m+1)}}{\partial \mu}(c)$ changes sign from negative to positive, hence forming isola structures. However, there are other kinds of periodic orbits in the allowed symbolic sequence (for example, RL^kR^{2m+1}), whose reversal is interrupted by the homoclinic points. Extending the above type of arguments to such cases will depend on the nature of the sequences and appears difficult.

As discussed in the introduction, one important feature of MMO systems is the dominance of the parameter windows of stable periodic orbits of RL^k type. Using Eq.(10), we show that the width of the parameter windows of these stable periodic orbits depend critically on the structure of the map as determined by Eqs.(1) and (2). In particular, we will show that the ratio of the widths of successive periodic windows of the RL^k type is decreasing. Consider Eq.(10) for k and $k+1$ stable periodic orbits. In comparison with the k-th periodic orbit, there is an extra term in the product arising from an iterate falling on the monotonically increasing arm. Since the μ value of the $(k+1)$-th periodic orbit is larger than that for k-th one, which in turn implies $f(c)$ has moved towards c, we have

$$\prod_{n=2}^{k-1} \frac{\partial f}{\partial x}(f^n(c)) < \prod_{n=2}^{k} \frac{\partial f}{\partial x}(f^n(c)). \tag{10}$$

Further, since $f(c)$ moves towards the critical point, $|\frac{\partial f}{\partial x}(f(c))|$ increases. Noting that $\frac{\partial^2 f^k}{\partial x^2}(c)$ is negative, whose magnitude increases with k (or μ), it implies that $f^{k+1}(x)$ exhibits a sharper minimum around c than that for the k-th periodic orbit. Assuming that the extent of the neighbourhood around $f^k(c)$ can be approximated by $F^k \sim \frac{\partial^2 f^k}{\partial x^2}(c)(x-c)^2/2$, the window width of the k-th periodic orbit can be approximated by the product of F^k and $\frac{\partial f^k}{\partial \mu}(c)$. Since $|F^k| < |F^{k+1}|$ and $\left|\frac{\partial f^k}{\partial \mu}(c)\right| < \left|\frac{\partial f^{k+1}}{\partial \mu}(c)\right|$, it clear that the window width of the k-th periodic orbit is larger than that of $(k+1)$ periodic orbit. Since the value at which the reversal of PD sequence of the type RL^k occurs depend on the secondary bifurcation parameter ξ, it is possible that there may not be a change in the sign of $\frac{\partial f^k}{\partial \mu}(c)$ beyond a certain value of k. (Note that if $\frac{\partial f^k}{\partial \mu}$ does not change sign, then, there cannot be a change in sign for $m > k$.) Thus, only a few periodic sates of RL^k would be seen. However, for the period adding sequences, the number of states of RL^k can go unbounded. For this case, a channel at small x should open up. The onset of a channel can be anticipated based on Eq. (1) which implies that the graph of the map comes down with μ, and $f(0, \xi, \mu) = a$, i.e., nonzero value as the origin of the map. A power series representation for the monotonically increasing part with conditions $f'(0, \mu, \xi) < 1$ and $f''(0, \mu, \xi) > 0$ ensures that there is one point to left of c that has $f'(x, \mu, \xi) = 1$ for all values of the parameter. Then, for RL^k periodic sequences, the window widths of periodic orbits of the type RL^k decreases slowly.

B. Scaling relations for periodic orbits

Having argued for the predominance of the periodic orbits of sequence of RL^k type in the parameter space, we show that periodic windows contained in the chaotic region bounded by the windows of periodic orbits denoted by RL^k and RL^{k+1} have much smaller parameter width compared to that of RL^k and RL^{k+1}. Numerical results on the map - L are also presented in support of the analytical result.

The PA sequence also manifest in NS-unimodal maps [37] as a part of MSS sequence[38]. In the MSS sequence, between any successive RL^{k-1} and RL^k windows, there exist windows of allowed sequences of the type $RL^k[S]$, where $[S]$ is a sequence consistent with the allowed symbol sequences[39], i.e.,

$$RL^{k-1} \prec \cdots \prec RL^k[S] \cdots \prec RL^k.$$

Considering only the increasing behaviour of long tailed maps, we assume that the MSS ordering corresponding to the periodic orbits of NS-unimodal maps may be applied for these types of maps also.

Let the bifurcation values $\tilde{\mu}_k$ correspond to the last generation k-period orbit in the MSS sequence, i.e., for

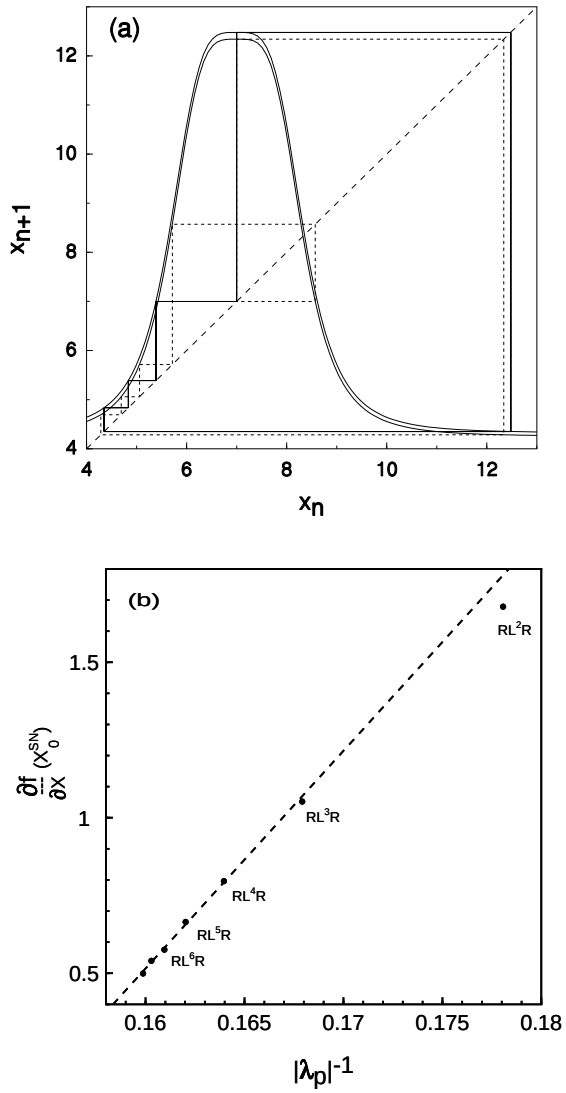

FIG. 6: (a) Map-L and the periodic orbit of form RL^3 and RL^4R for $\mu = 3.7831$ and $\mu = 3.99$ respectively ($\xi = 18.0$). (b) Verification of the scaling of $\frac{\partial f}{\partial x}(x_0^{SN})$ with $|\lambda_p|^{-1}$ for RL^nR periodic sequences obtained from the example Map-L. The dashed line is drawn for a linear fit.

$\mu > \tilde{\mu}_k$ no more cycles of period k are present. Thus, the parameter values are ordered in the following way:

$$\mu_3 = \tilde{\mu}_3 < \tilde{\mu}_3^h < \tilde{\mu}_4 < \tilde{\mu}_4^h < \tilde{\mu}_5 < \cdots$$

where $\tilde{\mu}_k^h$ refers to degenerate homoclinic bifurcation [40] (wherein $f^k(c) = p$) of the periodic point p between k-th and $(k+1)$-th periodic orbits.

Using a degenerate homoclinic bifurcation as the boundary, the parameter space for all the periodic windows between RL^{k-1} and RL^k (of period $k+1$ and $k+2$) can be divided into two regions, as $R_I : [\tilde{\mu}_{k+1}, \tilde{\mu}_{k+1}^h]$ and $R_{II} : [\tilde{\mu}_{k+1}^h, \tilde{\mu}_{k+2}]$. Consider the periodic window corresponding to the simplest symbolic sequence in the regions R_I where stable periodic windows are of the type $RL^kR[S]$. Within this sequence, the most dominant (in the sense of the MSS sequence) periodic sequence is RL^kR which has one period higher than the basic sequence RL^k. Using Eq.(5), for a $k-$th periodic orbit ($f^k(x_0) = x_0$), the eigen value of the periodic orbit, λ, is given by,

$$\lambda = \prod_{n=0}^{n=k-1} \frac{\partial f}{\partial x}(x_n) \tag{11}$$

and for stability $|\lambda| \leq 1.0$. (For the period one fixed point, we have $\lambda_p = \left|\frac{\partial f}{\partial x}(p)\right| < 1.0$ for $\mu \leq \mu_2$.) Within the first order, we approximate all iterates falling in the neighbourhood U of p as having the same slope as at p. In the case of long tailed maps, owing to the sharp nature of longtailed maps, $\left|\frac{df}{dx}(p)\right|$ is large, for $\mu > \mu_3$. For the sake of clarity, consider the sequence RL^kR which is part of the sequence $RL^kR[S]$ in R_I. Clearly, the structure of the map ensures that one iterate of this sequence belongs to U (see for example map-L in Fig. 6a). In the case of RL^kR sequence, $f^{k+2}(x_0)$ falls in neighbourhood U of p. Using Eq. (2) for stability of the periodic orbit,

$$\left|\frac{\partial f}{\partial x}(x_0)\frac{\partial f}{\partial x}(x_{k+2})\prod_{n=1}^{k+1}\frac{df}{dx}(x_n)\right| \leq 1.0 \tag{12}$$

where x_0 is an initial point chosen to be in the neighbourhood of the critical point for reasons that will become clear soon. Since long tailed maps are sharply peaked (Eqs.(1) and (2)), almost all the iterates are trapped in the intermittency channel like region near the origin of the map. (This point is best illustrated by considering the concrete example of map-L shown in Fig. 6a, where RL^3 and RL^4R are shown.) Thus, for large k, noting that iterates other than x_0 and x_{k+2} change only marginally, for stability of the periodic orbit, we have

$$C\left|\frac{\partial f}{\partial x}(x_0)\frac{\partial f}{\partial x}(x_{k+2})\right| \leq 1.0$$

where C ($= \prod_{n=1}^{k+1} f'(x_n)$) is a constant factor. Since x_{k+2} falls in the neighbourhood of $p \in U$, $\left|\frac{\partial f}{\partial x}(x_{k+2})\right| \sim |\lambda_p| (\gg 1.0)$. Hence,

$$\left|\frac{\partial f}{\partial x}(x_0)\right| \leq [C|\lambda_p|]^{-1}. \tag{13}$$

Recall that for any periodic orbit, one iterate is always located in the neighbourhood of the critical point in the interval $[x_0^{PD}, x_0^{SN}]$, where x_0^{SN} and x_0^{PD} correspond to the onset of the periodic orbit through a saddle node bifurcation at μ_n^{SN} and the destabilization of the periodic orbit through a period doubling bifurcation at μ_n^{PD}. As the parameter is increased from $\mu = \mu_n^{SN}$, the iterate x_0

can be regarded as traversing from x_0^{SN} to x_0^{PD}. Then, Eq. (14) implies that for the stability of the periodic orbit RL^kR, the iterate (x_0) is restricted to a smaller extent of the neighbourhood of the critical point than that corresponding to RL^k in order to compensate for the increase of $\left|\frac{\partial f}{\partial x}(x_{k+2})\right| \sim |\lambda_p|$. Assuming a uniform change in x_0 with respect to the parameter μ as it traverses from x_0^{SN} to x_0^{PD} and using the fact that $\lambda_p \gg 1.0$, the parameter windows of RL^kR is smaller by a factor λ_p than that for RL^k. Similar arguments can be used to show that any sequence with $2m+1$ extra visits to the right than RL^k would have a window width smaller by a factor $\lambda_p^{-(2m+1)}$. (The assumption here is that these visits to the right are close to p.) Since any $RL^kR[S]$ sequence consists of $2m+1$ right visits over and above the basic sequence RL^k, the width of this periodic window is vanishingly small for large m. Thus,

$$\left|\frac{\partial f}{\partial x}(x_0)\right| \leq C^{-1}\left|\lambda_p^{-(2m+1)}\right|. \tag{14}$$

More specifically, Eqs. (13) and (14) allows us to get a scaling relation between the onset of the periodic windows of type RL^kR^{2m+1} which can be verified by using the map-L. For this we fix the control parameter, μ at the fold bifurcation points of the periodic windows so that the equality holds in Eq. (14). Under this condition, Eq.(14) (for $m=0$) implies that $\left|\frac{\partial f}{\partial x}(x_0^{SN})\right| \lambda_p = C^{-1}$ which is almost independent of k in RL^kR. To verify this, we have plotted $\left|\frac{\partial f}{\partial x}(x_0^{SN})\right|$ as a function of $|\lambda_p|^{-1}$ which exhibits linear scaling behaviour for the onset values of RL^nR windows using the map-L (Fig. 6b). In a similar fashion, we have shown a plot of $\frac{\partial f}{\partial x}(x_0^{SN})$ as a function of $|\lambda_p|^{-(2m+1)}$ for various m values corresponding to periodic orbits of RL^2R^{2m+1} type (Fig. 7). Note that, even though large k approximation is used, the scaling relations work well when k is not large (Figs. 6b and 7).

In the region R_{II}, the allowed periodic orbits are made up of the sequence $RL^kR^2[S]$ which has at least two more iterates to the right than the corresponding RL^k orbit. (See Fig. 8a.) The smallest allowed periodic orbit in this region is RL^kR^2 which has exactly two iterates more than the periodic orbit RL^k both of which lie in the neighbourhood U of p. (Note that even though the actual distance of these iterates may be substantially away from p, due to sharpness of the map, the slopes at these points can be approximated by the slope at p.) Thus, approximating the derivatives of the map for these two iterates falling in the neighbourhood U of p to be λ_p, the eigen value of the periodic orbit RL^kR^2 is seen to increase by a factor λ_p^2 compared to RL^k orbit. Hence, we have

$$\left|\frac{\partial f}{\partial x}(x_0)\right| \leq C^{-1}.\,|\lambda_p|^{-2}. \tag{15}$$

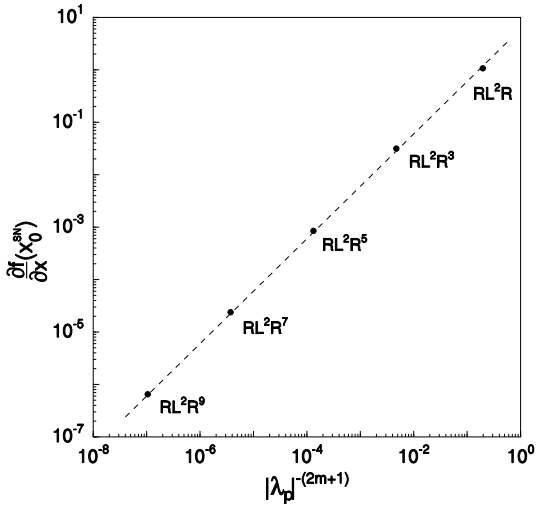

FIG. 7: Verification of the scaling of $\frac{\partial f}{\partial x}(x_0^{SN})$ with $|\lambda_p|^{-(2m+1)}$ for RL^2R^{2m+1} periodic sequences obtained from example Map-L.

Following arguments presented for R_I, we see that the iterate x_0 is restricted to a smaller extent around the critical point by a factor λ_p^{-2} which in turn leads to the width of RL^kR^2 being smaller by the same factor compared to RL^k. Using the equality, the above relation has been verified numerically for the map-L with the control parameter, μ, kept at the fold bifurcation point. Figure 8b shows the scaling for the onset of the periodic orbit RL^kR^2 with λ_p^{-2} which confirms the analytical result.

It is to be noted that in the chaotic region between RL^k and RL^{k+1}, there exist stable windows of other symbolic sequences also. In the above, the scaling is shown only for a particular sequence of periodic windows, namely RL^kR^m. However, the structure of the map ensures that any periodic orbit with periodicity higher than that of RL^kR and RL^kR^2 in the regions R_I and R_{II} respectively, typically have more number of iterates falling into the neighbourhood U of p. This structural feature along with the large value of λ_p ensures that the other window widths of these periodic orbits are increasingly small. //

III. CONCLUDING COMMENTS

One of main motivating factor for the study of a specific type of Poincare maps, namely the NMA maps, of MMO systems is that these maps constitute the dimensionally reduced form of the continuous time system; thus these maps are expected to retain all the key features of the MMO systems. It is well known that a dominant feature of homoclinic bifurcation to an

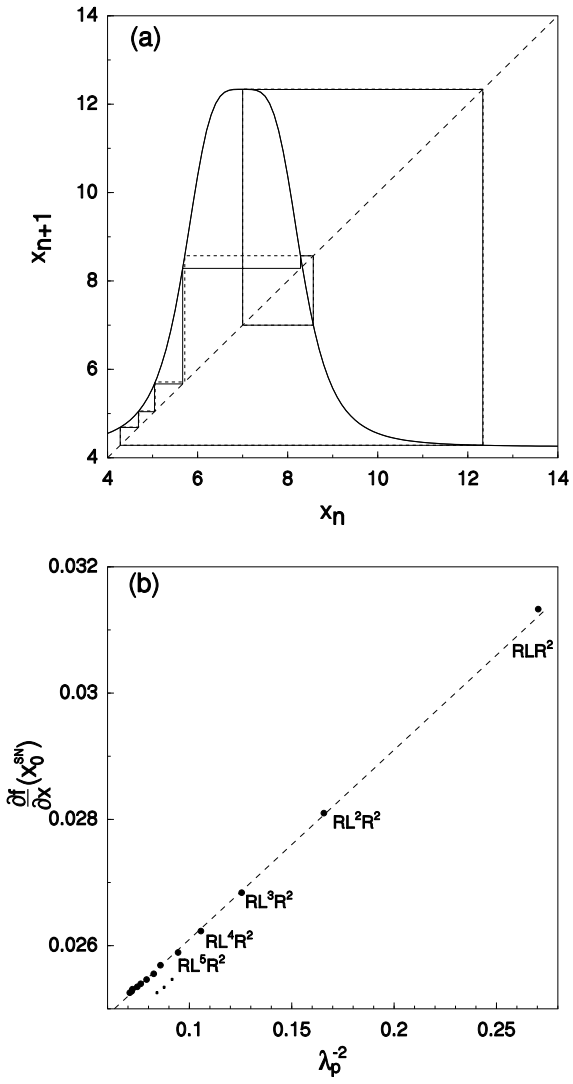

FIG. 8: (a) Periodic orbit sequence of RL^4R and RL^4R^2 for $\mu = 3.990345$ and $\mu = 4.001927$ for $\xi = 18.0$ for the Map-L (the maps are indistinguishable from each other on this scale). (b) Verifications of the scaling relation $\frac{\partial f}{\partial x}(x_0^{SN})$ with $|\lambda_p|^{-2}$ for RL^nR^2 periodic sequences obtained from Map-L.

unstable limit cycle (Gavrilov-Shilnikov scenario) [41] is the existence of isola structure. This is observed in the region of periodic-chaotic sequences in MMO systems, and even in those cases which show incomplete approach to homoclinicity [3, 4, 12]. (See below.) Since the isola structure is preserved at the level of long tailed NMA maps, as a part of the study of long tailed maps, we have undertaken to investigate the origin of these isolas by studying the reversal of bifurcation sequences (within the limited scope of RL^k type of orbits). For example, the RL^k sequences were shown to be created and subsequently destroyed through a fold bifurcation leading to isola structures. *Hence, in the parameter region where period adding sequences (of type RL^k) manifest, these isolas are prominent and an isola with larger periodicity is embedded within the isola with a lower periodicity leading to a progressively ordered structure of isolas.* This feature mimics the ordered structure of the isolas present in certain types of MMO systems.

From the point of view of continuous time systems, the reversal of period doubling sequences is a direct consequence of the back-to-back Hopf bifurcations in these systems [7, 11, 12]. For a two parameter dynamical system, a degenerate Hopf bifurcation gives rise to back-to-back Hopf bifurcations and the existence of the periodic orbits is confined to this interval in the parameter space. Within the region of back-to-back Hopf bifurcations, any bifurcation wherein periodic orbits are created has to be matched by a reverse bifurcation of the same kind wherein the periodic orbits will be destroyed. In other words, in these continuous flow systems also, the periodic orbits born in a fold bifurcation vanishes in another fold bifurcation creating an isola structure. Moreover, the amplitude of the period one orbit arising from the first Hopf bifurcation approaching the other Hopf bifurcation (while going from the periodic state to a fixed point) gets progressively smaller. Since the period one orbit is equivalent to a fixed point of the NMA map, this feature translates to the condition $\frac{\partial f}{\partial \mu}(p) < 0$ that has been imposed for the changes in the structure of the map. A consequence of this condition is that *the first period doubling occurs due to the changes in the shape of the map in the neighbourhood of period one fixed point, while the rest of the period doubling bifurcations are due to the presence of the critical point.* This difference in the cause of the first period doubling bifurcation and higher order bifurcations is reflected in the first Feigenbaum exponent being distinctly different from the rest of the PD bifurcations [17, 48]. Equivalently, a large period two window is seen as a distinct feature of the alternate periodic-chaotic sequences of MMO systems also.

We have shown that the increasing sharpness of the map and the consequent long tail nature, as the parameter is tuned, determines the dominance of the RL^k periodic states. Heuristically, the dominance of the RL^k type periodic orbits can be related to the arguments on dissipation in the following manner. The primary features of the structure of the map relevant to the predominance of period adding sequences is the large eigen value (in absolute terms) for the period one fixed point, the long tail structure, and the presence of an intermittency channel. In these class of maps, apart from the neighbourhood of the critical point, there exists a large tail region wherein the slope is small. By definition, these regions are related to high dissipation, since the spread of the iterates in its next iteration is suppressed. (Given an neighbourhood I_1 in the tail region, $I_2 = f(I_1; \mu, \xi) \ll I_1$.) One type of sequence of periodic orbits which include visits to the regions of

high dissipation with no visits to the neighbourhood containing p are the RL^k sequences. *High dissipation favours periodic orbits, hence the stability of these periodic sequences are enhanced at the expense of the chaotic regions.* In the same spirit, the windows of periodic orbits occurring within the chaotic region between any two successive RL^k sequences, involving at least one iterate in the neighbourhood of the unstable fixed point and favouring negative dissipation (local expansion) have window widths smaller by a factor of λ_p. These analytical results for the onset of periodic orbits of the type RL^kR^m show that the slope at the point of onset of the periodic orbit, namely $\frac{\partial f}{\partial x}(x_0)$ is related to the slope of the unstable fixed point λ_p, and scales linearly with λ_p^{-m}, where m is the number of visits to the neighbourhood of the unstable period one fixed point. *The relationship between the slopes near the critical point and the fixed point essentially controls the width of such periodic orbits. It must be emphasised that these scaling relations derived are very different from those usually derived where the widths of the periodic orbits are evaluated as a function of the parameters.* Again, map-L has been used *only* to verify these scaling relations. The scaling relation suggests that the width of the parameter window is nearly independent of the visits to the left of critical point of the map and only the visits to the neighbourhood of p determine the width of these type (RL^k) of periodic windows. For a map with a sharp maximum and a long tail, the eigen value of the unstable fixed point will be large and consequently smaller windows widths for the periodic orbits contained in the chaotic region sandwiched between RL^{k-1} and RL^k.

A necessary condition for the occurrence of the reversal of period doubling sequences in unimodal maps have been stated in the form of the first two conditions defined by Eqs. (1) and (2), which are constructed keeping in mind the changes in the structure of the NMA maps of the MMO systems. The correctness of these conditions is validated by the fact that the dominant bifurcation sequences of the long tailed maps and the MMO systems have similar features. Further, the similarity of the bifurcation diagrams obtained from the example map-L (belonging to the class of long tailed maps) is similar to the MMO systems and in particular bifurcation sequences from AK model. Since the dissipation involved in the higher dimensional continuous time is related to the separation of time scales operating in the system, a larger separation of time scales implies near one dimensional nature as well as the long tailed structure for the map. Since the scaling relations incorporate the essential ingredients of the structure of the map, namely, the property of long tail and the *strength of the unstable fixed point* (λ_p), the scaling relations derived for the one-D maps can be used as an effective check for the kind of dynamics involved in the higher dimensional systems. These observations are subject to usual criticism applicable to maps considered as reduced dynamical systems. In higher dimensional systems, it is conceivable that the interaction between several parameters can lead to reversal of period doubling and period adding sequences. The present work only attempts project the entire complexity into a few constraints. Clearly, these constraints on the maps can be satisfied in variety of combinations of parameters in higher dimensional space.

In summary, we have traced the dominance of period adding sequences as a part of complex alternate periodic-chaotic sequences in MMO systems to the long tailed nature of the associated Poincare maps. In the process, we have *partially* elucidated the origin of the reversal of the bifurcation sequences with specific reference to RL^k type of orbits which are the dominant sequences in MMO systems. *The results are derived based on some general conditions alone without taking recourse to any particular analytical form of the map*; the map-L is used only to numerically confirm the analytical results. Further, the example map-L which satisfies the general constraints mimics the distinctive features of higher dimensional continuous flow MMO systems, namely, the reversal of PD bifurcation sequences and the alternate periodic-chaotic sequences. The specific feature of the dominance of windows periodic orbits over the chaotic regions in the long tailed maps also captures the equivalent feature for the continuous time MMO systems. Since, many maps of experimental MMO systems exhibit generic features similar to those used here, the scaling relations derived for the onset of the periodic orbits of the form RL^kR^m can be taken to serve as a check for the correctness of the analysis. In particular, in BZ systems, while earlier experiments do show the dominance of the period adding sequences [29], the existing results are not accurate enough to verify these scaling relations. However, we believe that careful experiments should bear out our results. Indeed, we expect that careful experiments on a number of other experimental systems wherein the geometrical shape of the Poincare map is similar to Fig. 2 [6, 7, 8, 19], could be used to validate our results. Another example would be the laser systems where accuracy of control on parameters is generally considerably high. These results also indicate the ubiquity in the qualitative dynamical features of physical systems from widely differing origin, exhibiting alternate periodic-chaotic sequences.

IV. APPENDIX

In this appendix, we provide an example two parameter map which has the following broad typical features observed by the NMA maps of MMO systems: a) non zero origin, b) a sharp symmetric maximum positioned asymmetrically, and c) asymptotic long tail to the right of the maximum. It is a generalisation of the Bountis

map[30] given by

$$\begin{aligned} x_{n+1} &= f(x_n;\mu,\xi) \\ f(x;\mu,\xi) &= a + \frac{(\xi-\mu)+r(x-c)^l}{s_1+s_2\mu(x-c)^m} \end{aligned} \quad (A\text{-}1)$$

with $m \geq l$ and $a > 0$. We refer to this map given by Eq. (A1) as map-L. This map is used mainly to verify the analytical results derived in text. We shall use only two parameters μ and ξ of the several parameters l, m, a, r, s_1, s_2 and c. The other parameters of the map $f(x;\mu,\xi)$ are tuned such that the model map looks similar (in structure) to one dimensional maps of the MMO systems (Fig. 2). For our numerical study, we use the following values for the map parameters : $l = m = 4.0, a = 3.0, r = 0.6, s_1 = 1.5, s_2 = 0.12$ and $c = 7.0$. We shall use μ and ξ as primary and secondary bifurcation parameters respectively.

The bifurcation diagrams are constructed using μ as a control parameter for fixed value of ξ. Fig. 3 shows a typical shape of the map defined by Eq. (A1). This map has a unique smooth maximum with inflection points on either side of the maximum. For properly chosen initial conditions, the asymptotic tail ensures that the nontrivial dynamics of the map is restricted to the interval $[f^2(c;\mu,\xi), f(c;\mu,\xi)]$. It can be easily verified that the map has a negative Schwarzian derivative everywhere on the positive real line. Since $a > 0$, for an appropriate choice of a, there are no fixed points in the interval $[0, c]$ for small values of ξ. For a range of values of the parameter $\xi < \xi^*$, the map has only one fixed point, p, which is in the interval $[c, f(c)]$. For $\xi > \xi^*$, two more fixed points, p_2 and p_3, located in the interval $[0, c]$, are born in a fold bifurcation at $\mu = \mu^*(\xi)$. (Both p and p_3 are unstable, and p_2 is stable.)

In the following, we briefly describe the bifurcation sequences of the map $f(x;\mu,\xi)$ with respect to the primary bifurcation parameter μ for various values of ξ. For small but fixed value of ξ, an increase in the value of μ leads to a decrease in the value of p. For $\xi < 8.0$, the unique fixed point p is stable for all values of μ. Beyond $\xi = 8.0$, the fixed point p loses stability in a period doubling bifurcation as μ is increased which is regained in a period undoubling bifurcation thus forming a bubble structure (Fig. 4a). For further increase in ξ, the number of nested bubbles grows as 2^n with $n = 1, 2, 3 \cdots$. For $\xi \sim 11.9$, a period three window opens up in the bifurcation diagram separating the period doubling sequences from the reverse period doubling sequences (Fig. 4b). Further increase in the value of ξ unveils period adding sequences of arithmetically increasing periodic windows coexisting with the bubble structure (Fig. 5a). This sequence of large parameter windows of stable periodic orbits (in μ) is found to be of RL^k type sequences in the two letter symbolic dynamics language. For $\xi = 12.8$, we find that the reversal of the dominant bifurcation sequences occur beyond $\mu \sim 4.05$. At $\xi = 18.0$ ($\xi^* \sim 13.0$), as we increase μ, at $\mu = \mu^* = 4.8$, the region of the map for small values of x makes contact with the bisector giving rise to a fold bifurcation with the creation of a pair of stable and unstable fixed points, p_2 and p_3 (Fig. 5b). Keeping $\xi \geq \xi^*$, as the parameter μ is increased towards μ^*, the channel between the bisector and the map gets progressively narrow, thereby stabilising periodic orbits of higher periodicity (See Fig. 3 and also Figs. 6a,8a). The positions of the iterates of higher periodic cycles change marginally to accommodate the next higher periodic cycle as additional iterates are squeezed in this intermittent channel. Thus, the intermittency or the fold bifurcation point (μ^*) is an accumulation point for the arithmetically increasing period adding sequences. Beyond the accumulation point, no further bifurcations are observed for the stable periodic point (p_3). This map reproduces most bifurcations features of the AK model. (Compare bifurcation diagrams here with those in [12] and [48].)

Acknowledgments

One of the authors (R.R) gratefully acknowledge the financial support from Department of Science and Technology and partial financial support from Jawaharlal Nehru Center for Advanced Scientific Research.

[1] L. Gyorgi, R. J. Field, Z. Noszticzius, W. D. McCormick and H. L. Swinney, J. Chem. Phys. **96** 1228 (1992)
[2] D. Barkley, J. Chem. Phys. **89** 5547 (1988).
[3] V. Petrov, S.K. Scott, K. Showalter, J. Chem. Phys. 97, (1992) 6191.
[4] M.T.M. Koper, Physica D80 (1995) 72.
[5] A. Arneodo, F. Argoul, J. Elezgaray, P. Richetti, Physica D62 (1993) 134 *(and the references therein).*; J.S. Turner, J.-C. Roux, W.D. McCormick, H.L. Swinney, Phys. Lett. A85 (1981) 9; P. Ibibson, S. K. Scott, J. Chem. Soc. Faraday Trans. 87 (1991) 223; Z. Noszticzius, W.D. McCormick, H.L. Swinney, J. Phys. Chem. 93 (1989) 2796.
[6] F.N. Albahadily, J. Ringland, M. Schell, J. Chem. Phys. 90 (1989) 813.
[7] M.T.M. Koper, P. Gaspard, J. Chem. Phys. 96 (1992) 7797; M.T.M. Koper, P. Gaspard, J.H. Sluyters, J. Chem. Phys. 97 (1992) 8250.
[8] K. Krischer, M. Lubke, M. Eisworth, W. Wolf, J. L. Hudson, G. Ertl, Physica D62 (1993) 123.
[9] T. R. Chay, Y. S. Yan, and Y. S. Lee, Int. J. Bifur. Chaos **5** 595 (1995).
[10] T. Braun, J. A. Lisboa, Int. J. Bifur. Chaos **4** 1483 (1994).
[11] Ferdinando de Tamosi, D. Hennequin, B. Zambon, E.

Arimondo, J. Opt. Soc. Am. B6 (1989) 45.
[12] S. Rajesh and G. Ananthakrishna, Physica D140 (2000) 193; S. Rajesh and G. Ananthakrishna, Phys. Rev. E 61 (2000) 3664.
[13] M.J.B. Hauser, L.F. Olsen, J. Chem. Soc., Faraday Trans. 92 (1996) 2857.
[14] S. Rajesh, G. Ananthakrishna, Physica A270 (1999) 182.
[15] G. Ananthakrishna, M.C. Valsakumar, J. Phys. D15 (1982) L171. The basic model was formulated in G. Ananthakrishna, D. Sahoo, J. Phys. D14 (1981) 2081.
[16] L.N. Lorenz, J.Atmos. Sci. 20 (1963) 130.
[17] S. Rajesh, Ph. D Thesis, Indian Institute of Science, Bangalore (2000).
[18] K.G. Coffman, W.D. McCormick, H.L. Swinney, Phys. Rev. Lett. 56 (1986) 999; K.G. Coffman, W.D. McCormick, Z. Noszticzius, R. H. Simoyi, H.L. Swinney, J. Chem. Phys. 86 (1987) 119.
[19] M.R. Bassett, J.L. Hudson, J. Phys. Chem. 92 (1988) 6963; Y. Xu, M. Schell, J. Phys. Chem. 94 (1990) 7137; F. Argoul, J. Huth, P. Merzeau, A. Arneodo, H.L. Swinney, Physica D62 (1993) 170; T. Braun, J.A. Lisboa, Int. J. Bif. and Chaos 4 (1994) 1483; C.J. Doona, S.I. Doumbouya, J. Phys. Chem. 98, (1994) 513.
[20] J. Guckenheimer, P.J. Holmes, Nonlinear oscillations, Dynamical Systems and Bifurcations of Vector Fields, Springer, Berlin, 1990.
[21] P. Gaspard, R. Kapral, G. Nicolis, J. Stat. Phys. 35 (1984) 697.
[22] P. Glenndining, C. Sparrow, J. Stat. Phys. 35 (1984) 645.
[23] P. Gaspard, X.J. Wang, J. Stat. Phys. 48 (1987) 151.
[24] O. Michelin, P.E. Phillipson, Phys. Lett. A188 (1994) 309.
[25] H.P. Fang, Z. Phys. B 96 (1995) 547.
[26] R.H. Simoyi, A. Wolf, H.L. Swinney, Phys. Rev. Lett. 49 (1982) 245.
[27] R.J. Bagley, G. Mayer-Kress, J.D. Farmer, Phys. Lett. A114 (1986) 419.
[28] J. Ringland, J.S. Turner, Phys. Lett. A105 (1984) 93.
[29] A.S. Pikovsky, Phys. Lett. A85 (1981) 13.
[30] M. Bier, T.C. Bountis, Phys. Lett. A104 (1984) 239.
[31] H.E. Nusse, J.A. Yorke, Phys. Lett. A127 (1988) 328.
[32] U. Parlitz, W. Lauterborn, Phys. Lett. A107 (1985) 351; Phys. Rev. A36 (1987) 1428.
[33] I. Kan, H. Kocak, J.A. Yorke, Ann. Math. 136 (1992) 219.
[34] S.P. Dawson, C. Grebogi, J.A. Yorke, I. Kan, H. Kocak, Phys. Lett. A162 (1992) 249; S.P. Dawson, C. Grebogi, H. Kocak, Phys. Rev. E48 (1993) 1676.
[35] J. Ringland, N.Issa, M. Schell, Phys. Rev. A41 (1990) 4223.
[36] M. Schintuchand and Schimdt, J. Phys. Chem. **92** 3404 (1988).
[37] T. Geisel, J. Nierwetberg, Phys. Rev. Lett. 47 (1981) 975.
[38] N. Metropolis, M.L. Stein, P.R. Stein, J. Comb. Theory 15 (1973) 25.
[39] T. Post, H.W. Capel, Physica A178 (1991) 62.
[40] L. Gardini, Nonlinear Anal., Theory, Methods and App. 23 (1994) 1039.
[41] N.K. Gavrilov, L.P. Shilnikov, Mat. USSR Sb. 17 (1972) 467; 19 (1973) 139.
[42] B.D. Aguda, R. Larter, J. Am. Chem. Soc. 113 (1991) 7913.
[43] T.C. Newell, V. Kovanis, A. Gavrielides, P. Bennet, Phys. Rev. E54 (1996) 3581.
[44] K. Tomita, I. Tsuda, Prog. Theo. Physics 64 (1980) 1138.
[45] K. Kaneko, Prog. Theor. Phys. 68 (1982) 669; K. Kaneko, Prog. Theor. Phys. 69 (1983) 403.
[46] A.B. Corbet, Phys. Lett. A130 (1988) 267.
[47] H.L. Swinney, Physica D7 (1983) 3; K. Coffman, W. D. McCormick, H.L. Swinney, Phys. Rev. Lett. 56 (1986) 999.
[48] G. Ananthakrishna, T. M. John, in: Hao Bai-Lin (Ed.), Directions in chaos, World Scientific, Singapore, 1990.
[49] Even as Eq.1 implies that the whole map is coming down uniformly, Eq.2 constrains the rate of change to be different in different regions of the map.